

QFAST: Conflating Search and Numerical Optimization for Scalable Quantum Circuit Synthesis

Ed Younis*, Koushik Sen[†], Katherine Yelick[†], Costin Iancu*

**Computational Research Division*

Lawrence Berkeley National Laboratory

[†]Department of Electrical Engineering and Computer Science

University of California Berkeley

Berkeley, CA

Abstract—We present a quantum synthesis algorithm designed to produce short circuits and to scale well in practice. The main contribution is a novel representation of circuits able to encode placement and topology using generic “gates”, which allows the QFAST algorithm to replace expensive searches over circuit structures with few steps of numerical optimization. When compared against optimal depth, search based state-of-the-art techniques, QFAST produces comparable results: $1.19\times$ longer circuits up to four qubits, with an increase in compilation speed of $3.6\times$. In addition, QFAST scales up to seven qubits. When compared with the state-of-the-art “rule” based decomposition techniques in Qiskit, QFAST produces circuits shorter by up to two orders of magnitude ($331\times$), albeit $5.6\times$ slower. We also demonstrate the composability with other techniques and the tunability of our formulation in terms of circuit depth and running time.

1. Introduction

Quantum synthesis techniques generate circuits from high level mathematical descriptions of an algorithm. Thus, they can provide a very powerful tool for circuit optimization, hardware design exploration and algorithm discovery. An important quality metric of synthesis and compilers in general is circuit depth, as it relates directly to the program performance. Short depth circuits are especially important for Noisy Intermediate Scale Quantum (NISQ) era devices, characterized by limited coherence time and noisy gates: here synthesis can morph from a capacity into a capability provider.

Synthesis has a long and distinguished research history [4], [5], [18], [19], [20], [22], [25], [31], [33], [45], [49]. At one end of the spectrum, optimal depth algorithms have been introduced for two qubits [49] (KAK), augmented very recently with search based techniques [18] that “scale”¹ up to four qubits. The latter employ a bottom-up approach, where the solution circuit is extended one layer at a time while taking into account the physical topology of the target Quantum Processing Unit (QPU). At the other end

of the spectrum, top-down approaches [25], [45] use a “rule” based, divide-and-conquer decomposition approach. An exponent technique is deployed in IBM Qiskit [1], which uses linear algebra inspired, top-down decomposition. While more scalable, top-down techniques lack a good solution for topology awareness and tend to generate much longer (orders of magnitude) circuits than the slower optimal techniques.

The behavioral quality of optimal techniques is determined by several factors. The search algorithm determines the number of partial solutions evaluated: any strategy to reduce these will improve scalability. Each partial solution is subject to numerical optimization, which in turn scales exponentially with the number of parameters and it is greatly affected by the formulation of the objective function. Thus, these bottom-up techniques slow down the closer they get to a solution. Furthermore, topology awareness greatly reduces the final solution depth.

Quantum Fast Approximate Synthesis Tool (QFAST) has been designed to improve scalability by trading-off search computational complexity with numerical optimization complexity. It implements a bottom-up approach, whose main contribution comes from encoding and using “powerful” computational building blocks. Most search based techniques [18] use simple 2-qubit parameterized blocks that contain two $U3$ gates and a two-qubit gate, usually $CNOT$ ².

In contrast, QFAST can use arbitrary generic gates applied to any arbitrary set of qubits. The generic gates in QFAST encode *function*, i.e. the quantum transformation performed by the gate, together with *location*, i.e. the set of qubits operated on. QFAST uses a three stage topology aware hierarchical algorithm. First, the circuit is built bottom-up by adding one generic gate at a time. For a n -qubit input algorithm, we start by adding m -qubit generic gates, $m < n$. Initially, this gate encodes the application of any m -qubit program on any subset of m qubits from the original n -qubit circuit. A numerical optimization subroutine specializes the gate to a certain computation on a single set of m -qubits such as we make most progress to solution (minimize a unitary distance function). The process contin-

1. Compilation finishes in a “reasonable” amount of time.

2. For superconducting qubits.

ues hierarchically until reaching a size for “ m ”-qubit gates. Then these can be passed and handled by third-party native synthesis tools. The last stage of QFAST is hierarchically reassembling the circuit using the native implementation of each generic gate added in the first stage.

The three stage approach in QFAST enables composability and tunability of approximations. First, we can plug in any native synthesis tool, at any qubit concurrency, based on its perceived quality of solution or execution speed. Second, we can decouple the “distance” metrics in the generic gate space from the distance metrics in the native gate space, thus enabling finer approximations of the input circuit.

QFAST has been evaluated on a series of algorithms used in previous synthesis and circuit mapping studies [8], [15], [17], [37], [38]. We compare its performance directly against the QSearch [18] optimal algorithm and against the IBM Qiskit synthesis [1] modules. To demonstrate composability, we show experiments when leveraging two-qubit native optimal depth KAK decomposition, two- and three-qubit Qsearch.

The results indicate that QFAST behaves well in practice. When compared against depth optimal synthesis in QSearch on circuits up to four qubits, QFAST produces circuits on average $1.19\times$ longer with an average reduction in execution time of $3.55\times$. QFAST scales up to seven qubits. When compared against the synthesis algorithms deployed in IBM Qiskit, QFAST produces circuits on average $156\times$ shorter, albeit with an average time penalty of $15\times$. When compared directly against traditional compilation approaches in IBM Qiskit, the QFAST circuits are on average $10\times$ shorter.

The rest of this paper is organized as follows. In Section 2 we introduce the problem, motivation and provide a short primer on quantum computing. In Section 3 we describe our circuit encoding used in the algorithm, which is described in Section 4. We include an evaluation in Section 5 and a discussion in Section 6. Finally, we present related works in Section 7 and conclude in Section 8

2. Background

In quantum computing, a qubit is the basic unit of quantum information. Their general quantum state is represented by a linear combination of two orthonormal basis states (basis vectors). The most common basis is the equivalent of the 0 and 1 values used for bits in classical information theory, respectively $|0\rangle = \begin{pmatrix} 1 \\ 0 \end{pmatrix}$ and $|1\rangle = \begin{pmatrix} 0 \\ 1 \end{pmatrix}$.

The generic qubit state is a superposition of the basis states, i.e. $|\psi\rangle = \alpha|0\rangle + \beta|1\rangle$, with complex amplitudes α and β such that $|\alpha|^2 + |\beta|^2 = 1$.

The prevalent model of quantum computation is the circuit model introduced by Deutsch [21], where information carried by qubits (wires) is modified by quantum gates, which mathematically correspond to unitary operations. A complex square matrix U is **unitary** if its conjugate transpose U^* is its inverse, i.e. $UU^* = U^*U = I$.

In the circuit model, a single qubit gate is represented by a 2×2 unitary matrix U . The effect of the gate on the

qubit state is obtained by multiplying the U matrix with the vector representing the quantum state $|\psi'\rangle = U|\psi\rangle$.

The most general form of the unitary for a single qubit gate is the “continuous” or “variational” gate representation.

$$U_3(\theta, \phi, \lambda) = \begin{pmatrix} \cos\frac{\theta}{2} & -e^{i\lambda}\sin\frac{\theta}{2} \\ e^{i\phi}\sin\frac{\theta}{2} & e^{i\lambda+i\phi}\cos\frac{\theta}{2} \end{pmatrix}$$

A quantum transformation (algorithm, circuit) on n -qubits is represented by a unitary matrix U of size $2^n \times 2^n$. A circuit is described by an evolution in space (application on qubits) and time of gates. Figure 1 and 2 shows a few examples of circuit.

Circuit Synthesis: The goal of circuit synthesis is to decompose unitaries from $U(2^n)$ into a product of terms, where each individual term (e.g. from $U(2)$ and $U(4)$) captures the application of a quantum gate on individual qubits. The quality of a synthesis algorithm is evaluated by the number of gates in the circuit it produces and by the distinguishability of the solution from the original unitary.

Circuit length provides one of the main optimality criteria for synthesis algorithms: shorter circuits are better. CNOT count is a direct indicator of overall circuit length, as the number of single qubit generic gates introduced in the circuit is proportional with a constant given by decomposition (e.g. $ZZXZXZ$) rules. As CNOT gates have low fidelity on NISQ devices, state-of-the-art approaches [18], [26], [46] directly attempt to minimize their count. Longer term, single qubit gate count is likely to augment the quality metric for synthesis.

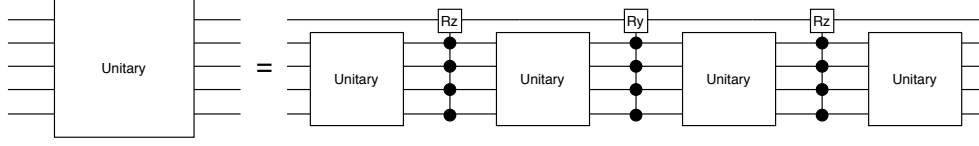
Synthesis algorithms use distance metrics to assess the solution quality, and their goal is to minimize $\|U_T - U_C\|$, where U_T is the unitary that describes the target transformation and U_C is the computed solution. They choose an error threshold ϵ and use it for convergence, $\|U_T - U_C\| \leq \epsilon$. Early synthesis algorithms use the diamond norm, while more recent efforts [18], [29], [30] use the Hilbert-Schmidt inner product between the conjugate transpose of U_T and U_C . This is motivated by its lower computational overhead.

$$\langle U_T, U_C \rangle_{HS} = \text{Tr}(U_T^\dagger U_C) \quad (1)$$

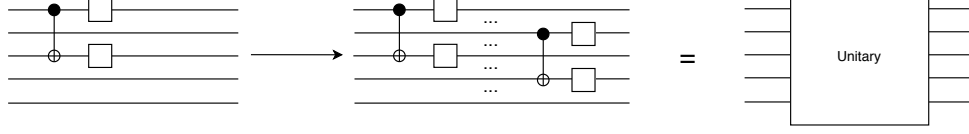
Top-Down Synthesis: These algorithms follow prescribed, simple rules to decompose large unitaries into a tensor product of smaller terms or into a product of symmetric matrices. Figure 1a illustrates the Quantum Shannon Decomposition (QSD) [45], which breaks an n -qubit unitary into four $(n-1)$ -qubit unitaries and three multi-controlled rotations. Like most top-down methods, synthesis with QSD is quick, but circuit depth grows exponentially. Overall, these techniques are memory limited, rather than computationally limited.

The only known depth optimal rule based algorithm is the KAK-decomposition [49], which is valid only for two-qubit operations. Due to its optimality, KAK has been used in both bottom-up and top-down compilers. For example, UniversalQ [27] implements multiple top-down methods, some exposed directly by IBM Qiskit. Their version of QSD stops when reaching two-qubit blocks which are instantiated to native gates by KAK.

Bottom-Up Synthesis: These algorithms, described in Fig-



(a) Top-down synthesizers follow prescribed, simple rules to decompose large unitaries into smaller ones while maintaining equality.



(b) Bottom-up synthesizers start with an empty circuit and build up to equality.

Figure 1: Quantum synthesizers are either top-down or bottom-up.

ure 1b, start with an empty circuit and attempt to place simple building blocks until equality is formed.

QSearch [18] introduces an optimal depth, topology aware synthesis algorithm that has been demonstrated to be extensible across native gate sets (e.g. $\{R_X, R_Z, CNOT\}$, $\{R_X, R_Z, SWAP\}$) and to multi-level systems such as qutrits. The approach employed in QSearch is canonical for the operation of other synthesis approaches that employ numerical optimization.

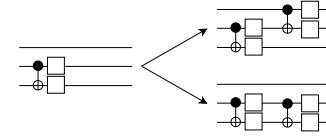
Conceptually, the synthesis problem can be thought as a search over a tree of possible circuit structures. A search algorithm provides a principled way to walk the tree and evaluate candidate solutions. For each candidate, a numerical optimizer instantiates the function (parameters) of each gate in order to minimize some distance objective function.

QSearch works by extending the circuit structure a layer at a time. At each step the algorithm places a 2-qubit expansion operator in all legal placements. For the CNOT gate set, the operator contains one CNOT gate and two $U3(\theta, \phi, \lambda)$ gates. QSearch then evaluates these candidates using numerical optimization to instantiate *all* the single qubit gates in the structure. An A* [24] heuristic determines which of the candidates is selected for another layer expansion, as well as the destination of backtracking steps. Figure 2a illustrates this process for a three qubit circuit.

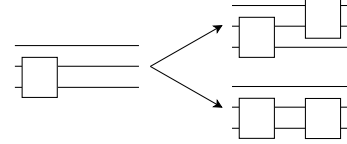
Although theoretically able to solve for any circuit size, the scalability of QSearch is limited in practice to four qubit programs due to several factors. The A* strategy determines the number of solutions evaluated: at best this is linear in depth, at worst it is exponential. Our examination of QSearch performance indicates that its scalability is limited to four qubits first due to the presence of too many deep backtracking chains. Any technique to reduce the number of candidates, especially when deep, is likely to improve performance.

As each expansion operator has two single-qubit gates, accounting for six³ parameters, circuit parameterization grows linearly with depth. Numerical optimizers scale at best with a very high degree polynomial in parameters, making optimization of long circuits challenging.

3. In practice, QSearch uses 5 parameters due to commutativity rules between single qubit and CNOT gates.



(a) QSearch uses native gates in synthesis and searches for structure in their circuit space. Each node in their circuit space is a valid circuit structure that has edges to circuits deeper by a 2-qubit native gate.



(b) QFAST uses block unitary matrices of arbitrary size. In this figure, 2-qubit blocks are used and a similar tree is constructed.

Figure 2: The 2-qubit unitary blocks are more expressive than one, fixed two-qubit gate followed by single-qubit rotations; Nodes 2 levels deep in the unitary block tree can only be expressed with nodes 6 levels deep in the native gate tree.

QFAST Approach: From the above discussion, several things become apparent. Top-down methods scale to a larger number of qubits than search based methods, and the quality of their solution can be improved by the introduction of (nearly) optimal depth techniques that work on more than two-qubits. The higher the number of qubits handled by the bottom synthesis, probably the higher the impact on the quality of the solution. Optimal search based techniques are limited in scalability first by the search algorithm, second by the scalability of numerical optimization. QFAST improves the synthesis scalability while providing good solutions through very simple intuitive principles:

- 1) As small two-qubit building blocks may lack “computational power”, we use generic blocks spanning a configurable number of qubits. See Figure 2b for an example of the tree with two-qubit building blocks. In this example, a depth *two* partial solution could express circuits that are up to depth *six*⁴ in

4. Any generic 2 qubit unitary expands in at most three CNOT gates, per KAK.

the Qsearch tree.

- 2) As the number of partial solutions and their evaluations may hamper scalability, we conflate the numerical optimization and search problem. We do this by using a continuous circuit space. At each step, the circuit is expanded by one layer. Given an n -qubit circuit, a layer encodes an arbitrary m -qubit operation on any m -qubits, with $m < n$. Thus, our formulation does not have a branching factor and solves combinatorially less optimization problems.

3. Gate and Circuit Representations

QFAST models a circuit as a sequence of parameterized gates. Each gate has a function (hence a size), and a location.

The function encodes the operation (quantum transformation) performed on an associated number of qubits. When operating with a gate whose function is parameterized, we refer to it as a *variable function gate*. Whenever gate parameterization is numerically instantiated, the gate becomes *fixed function*.

The location describes the set of qubits a gate is applied on, as placed in a larger circuit. A *variable location* m -qubit gate is associated with a set of n -qubits, $n > m$. In this case the gate can be applied to any valid subset of m -qubits from the total n -qubits defined by the target topology. A *fixed location* m -qubit gate operates on exactly m -qubits.

The QFAST algorithm uses two parameterizations: *variable function with fixed location* gates, and *variable function with variable location* gates. The second parameterization allows us to conflate search and optimization. In this section, we first describe how we encode gate variable function in a fixed size gate. Then we build on the function encoding to encode variable location.

3.1. Encoding of Gate Function

A gate's function is given by a unitary matrix. As such, encoding gate function is equivalent to structuring the unitary group. Conveniently, the unitary group $U(2^n)$ is a Lie group. Its Lie algebra $\mathfrak{u}(2^n)$ is the set of $2^n \times 2^n$ skew-Hermitian matrices. Using the Pauli group as generators for Hermitian matrices, we can construct the unitary group in the following way:

$$U(2^n) = \{e^{i(\vec{\alpha} \cdot \vec{\sigma}^{\otimes n})} \mid \vec{\alpha} \in \mathbb{R}^{4^n}\}$$

where $\vec{\sigma} = \{\sigma_x, \sigma_y, \sigma_z\}$ are the Pauli matrices, and $\vec{\sigma}^{\otimes n} = \{\sigma_j \otimes \sigma_k \mid \sigma_j \in \vec{\sigma}, \sigma_k \in \vec{\sigma}^{\otimes n-1}\}$ are the n -qubit Pauli strings.

This provides a useful parameterization of unitary operations on n -qubits. We can then define an n -qubit gate's function with 2^n parameters as:

$$G(\vec{\alpha}) = e^{i(\vec{\alpha} \cdot \vec{\sigma}^{\otimes n})}$$

This unitary-valued function is smooth and infinitely-differentiable. Its derivative is given by the derivative of the

exponential map [43], but when evaluating QFAST, we used the Padé approximation method with scaling and squaring [11] to compute the derivative.

3.2. Encoding of Gate Location

A gate's location determines which qubits it affects. One simple way to encode a fixed location is to map the Pauli strings that define the gate function to higher-order ones.

Given Q a fixed m -qubit location on an n -qubit circuit — a m -length sequence of qubit indicies that are all less than n — we define a map from m -qubit Pauli strings to n -qubit Pauli strings:

$$\pi_Q : \vec{\sigma}^{\otimes m} \longrightarrow \vec{\sigma}^{\otimes n}$$

This map inserts $n - m$ identities into the m -qubit Pauli string in positions not specified in the location. For example, if we are given a 2-qubit location $Q = (0, 1)$ on a 3-qubit circuit, then $\pi_Q(XX) = XXI$. If instead, $Q = (0, 2)$, then $\pi_Q(XX) = XIX$.

This leads to a parameterization of an m -qubit gate with variable function and a fixed location on an n -qubit circuit.

$$F(Q, \vec{\alpha}) = \exp(i(\vec{\alpha} \cdot \pi_Q(\vec{\sigma}^{\otimes m})))$$

If instead of a fixed location, we want variable location, given a set of valid locations, we can simply multiplex all possible locations. For example, if we want a formulation of a gate with variable function that affects either qubits $Q_0 = (0, 1)$ or qubits $Q_1 = (1, 2)$, we simply write:

$$\exp(i[l_0(\vec{\alpha} \cdot \pi_{Q_0}(\vec{\sigma}^{\otimes m})) + l_1(\vec{\alpha} \cdot \pi_{Q_1}(\vec{\sigma}^{\otimes m}))])$$

Here either l_0 or l_1 is 1 and the other is 0. If l_0 is one, then the formulation chooses the location given by Q_0 . Likewise, if l_1 is one, then the formulation chooses the location given by Q_1 . This can be extended to any number of possible locations \vec{Q} :

$$V(\vec{Q}, \vec{\alpha}, \vec{l}) = \exp(i \sum_{Q \in \vec{Q}} l_Q \cdot \vec{\alpha} \cdot \pi_Q(\vec{\sigma}^{\otimes m}))$$

3.3. Direct Mapping of Pauli Strings

Using the variable function with fixed location $F(Q, \vec{\alpha})$ and the variable location and function $V(\vec{Q}, \vec{\alpha}, \vec{l})$ gates, it is enough to implement an algorithm that replaces search with numerical optimization as shown in our first unpublished version of QFAST [54], [55].

In this formulation, we solve a mixed integer-real optimization problem, where the location and the associated

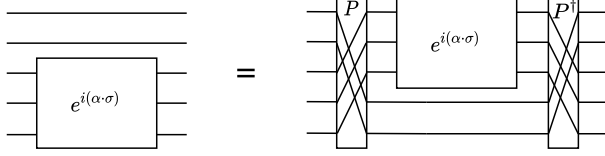


Figure 3: *Permutations can be used to encode location. A gate acting on the last 3-qubits of a 5-qubit circuit can be represented by a gate acting on the first 3-qubits preceded and followed by a permutation.*

discrete \vec{l} values are continuously approximated using the softmax [9] function⁵.

While the resulting implementation was able to produce good quality circuits, its scalability and numerical stability proved more challenging. First, the matrices $\pi_Q(\sigma^{\otimes m})$ are as large as the full circuit unitary rather than the gate’s unitary. Second, there are 4^m of these unitaries. This latter point is worse in the variable location model, where there are $|\vec{Q}|$ groups of 4^m full-sized matrices. The large dimensionality problem proved challenging to existing optimization packages, thus the algorithm was numerically unstable.

3.4. Permutations and Locations

We can sidestep these problems by using permutation matrices. This is because there exists a permutation matrix P_Q such that

$$F(Q, \vec{\alpha}) = P_Q(G(\vec{\alpha}) \otimes I)P_Q^T$$

This is illustrated in Figure 3. Now $F(Q, \vec{\alpha})$ uses the gate’s unitary in the equation and as such is much less costly to represent. The size of the Pauli matrices are now gate-sized rather than full-sized. This reduces the size of the model by an exponential factor.

Similarly, we can write the variable location model by multiplexing the permutation matrices rather than groups of Pauli matrices:

$$V(\vec{Q}, \vec{\alpha}, \vec{l}) = \left(\sum_{Q \in \vec{Q}} l_Q \cdot P_Q \right) (G(\vec{\alpha}) \otimes I) \left(\sum_{Q \in \vec{Q}} l_Q \cdot P_Q^T \right)$$

This formulation does use $|\vec{Q}|$ full-sized permutation matrices; however, since we do not need $|\vec{Q}|$ groups of pauli matrices, this is exponentially less costly than the variable location encoding using mapped Pauli strings. The resulting complexity of the model given by the number of parameters is $4^m + |\vec{Q}|$.

4. Synthesis Algorithm

QFAST’s uses a hierarchical synthesis algorithm split into three stages, as described in Figure 4. First, the target unitary is decomposed into parameterized unitary gates using the permutation model described in section 3.4 and the process described in Section 4.1. Next, the parameterized unitary gates are instantiated into native gates through the use of a third-party synthesis tool, as described in Section 4.2. As any native synthesis tool can be selected, this composability allows us to tune the quality of the solution together with the synthesis execution speed. Finally, the circuit is recombined into the final solution as described in Section 4.3.

4.1. Decomposition

Starting with an empty circuit, decomposition adds parameterized unitary gates layer by layer until the circuit is close to the target unitary. During construction, a partial solution contains only variable function with fixed location gates. At each step, the algorithm extends the partial solution with a single variable function with variable location gate, as illustrated in Figure 5. The new candidate is then passed to a gradient-based optimizer, which solves for the parameters. In doing so, the optimizer solves for the function of all gates and the location of the “head” gate. As a result, the variable-location gate has becomes a fixed-location gate. The process repeats until convergence, specified as a threshold on the distance between the target unitary and the partial solution.

Numerical optimization can easily encounter plateaus and local minima due to the complexity of the circuit and its associated objective function. During decomposition this manifests as the new candidate solution having a larger distance from target than the previous one. QFAST alleviates this by repeating the same operation/optimization with a more restricted topology for the head gate. In this case, the location that was chosen by the optimizer is removed from the possible locations for the head gate. We perform this action because choosing location seems harder for optimizers than solving only for gate function.

Decomposition transforms a target unitary into a circuit of smaller-sized unitaries. A benefit of using general unitary gates during decomposition, is that the process can be applied recursively. This gives a hierarchical decomposition algorithm.

4.2. Instantiation

The decomposition stage produces a candidate circuit composed of variable function blocks. While these can

5. The softmax function takes as input a vector z of K real numbers, and normalizes it into a probability distribution consisting of K probabilities proportional to the exponentials of the input numbers. That is, prior to applying softmax, some vector components could be negative, or greater than one; and might not sum to 1; but after applying softmax, each component will be in the interval $(0, 1)$, and the components will add up to 1, so that they can be interpreted as probabilities. Furthermore, the larger input components will correspond to larger probabilities.

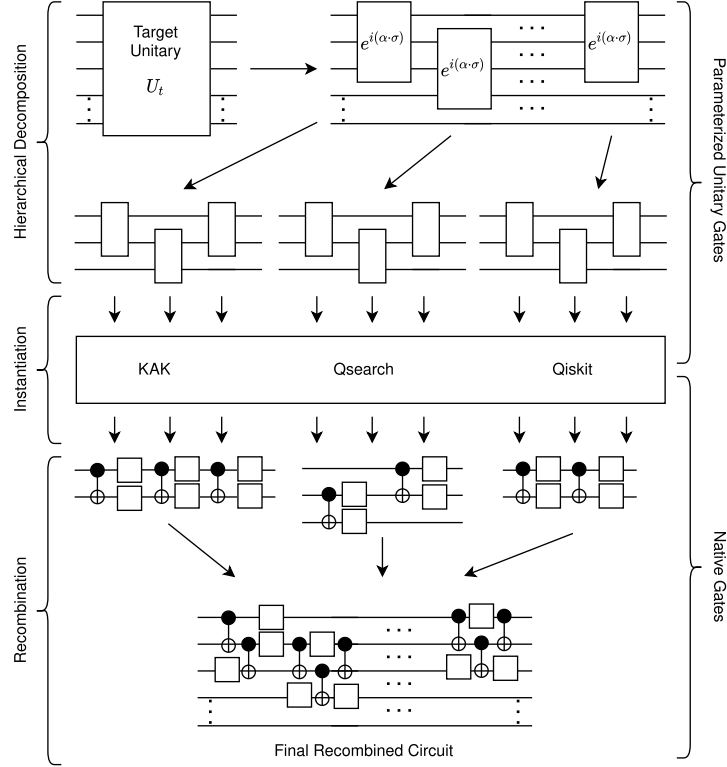


Figure 4: *QFAST* is broken down into three phases. In the first phase, decomposition, the target unitary is hierarchically broken down into smaller blocks. Up until this point, the gates are represented using the gate models described in section 3. During the next phase, instantiation, the block unitary gates are converted into native gates with third-party synthesis tools like *Qsearch* or with the KAK decomposition. Finally, during recombination the circuit is pieced back together and optimized where possible.

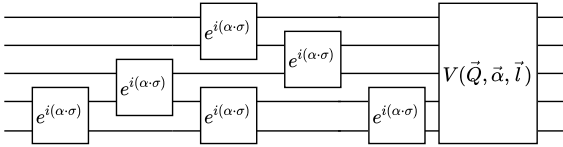


Figure 5: *Decomposition step in QFAST*. Variable function with variable location gates are appended to a prefix circuit formed of variable function with fixed location gates. A step of numerical optimization will convert the newly added gate to a variable function with fixed location gate.

perform any computation, they are not directly executable on hardware and we need a stage where blocks are transformed and rewritten into hardware native gates. This is the stage where we can freely leverage previous approaches and plug in any third-party synthesis tool. This composability gives *QFAST* portability across hardware architectures.

Although any solution can be used at this stage, the obviously mandatory choices are optimal depth topology aware algorithms: KAK [49] decomposition for two-qubit blocks and *QSearch* for three-qubit blocks.

4.3. Recombination

Finally, the recombination stage will stitch together into a complete circuit all the sub-circuits produced during *instantiation*, each associated with a variable function gate.

There is the opportunity to apply circuit optimization techniques during this stage. During instantiation, third-party synthesis tools are responsible for optimizing the native gate sequence for each block. Recombination is responsible for putting the circuit together, but there is also an opportunity here to optimize the native gate sequence across block boundaries. We use traditional gate-level optimization techniques to cancel or combine gates across block boundaries.

4.4. Distance Function

The goal of synthesis is to generate a circuit that implements a unitary U_C such that $\|U_T^\dagger U_C - I\| \leq \epsilon$, where the U_T is the target unitary, ϵ is some small number, I is the identity matrix. If ϵ is 0, or equivalent to machine floating point epsilon, then the synthesis is said to be exact, otherwise it is approximate.

The Frobenius norm $\|U_T^\dagger U_C - I\|$ is equivalent to $2 - 2\text{Re}(\text{Tr}(U_T^\dagger U_C))$. The above equation can be simplified and scaled in the context of synthesis to the following:

$$\Delta_F(U_C, U_T) = 1 - \frac{\text{Re}(\text{Tr}(U_T^\dagger U_C))}{d}$$

However, the Δ_F function is not tolerant of global-phase. Global-phase is irrelevant in quantum computation because it does not affect measurement. Being tolerant of

global-phase implies that equivalent unitaries up to global phase have zero distance. Δ_F can determine that two such unitaries have arbitrary large distance. The function can be made global-phase tolerant:

$$\Delta(U_C, U_T) = 1 - \frac{|Tr(U_T^\dagger U_C)|}{d}$$

We use the above as our cost function during optimization. A value of zero implies U_C and U_T are equivalent, and the largest value possible is one, which implies the unitaries are very far apart.

5. Evaluation

Software Implementation: QFAST is implemented in Python 3 using SciPy’s implementation of the L-BFGS [13] optimization algorithm. The `qfast` package is made available as part of the BQSKit tool suite through PyPI [2] and source code can be found at <http://github.com/BQSKit/qfast>. The software accepts as input a target unitary matrix, and the output is presented to users as an OpenQASM 2.0 [16] circuit/program. The following evaluation was performed on a desktop computer with a 3.3GHz AMD 2950X processor with 16 cores for a total of 32 threads.

Benchmarks: The benchmark suite is composed of third party algorithms used by other evaluation studies [8], [15], [17], [37], [38]. We consider circuits with known optimal implementations, such as Quantum Fourier Transform [40], HHL [23] and important quantum kernels such as Toffoli gate, multiplier, adder etc. These allow us to gauge the optimality of our solution.

We also consider circuits from domain generators such as the Variational Quantum Eigensolver [35] (VQE) or Transverse Field Ising Models [7], [8], [47] (TFIM). TFIM is an exponent of chemical simulations using time dependent Hamiltonians. In this case, domain-specific compilers repeat a fixed function ansatz for every timestep and circuit depth grows linearly. Domain tools concentrate in reducing ansatz depth and can’t avoid linear growth. As no optimal depth circuit is known for these algorithms, they allow us to showcase the benefits of synthesis for circuit optimization.

Comparison with State-of-the-Art: We evaluate QFAST alongside state-of-art bottom-up and top-down synthesis tools, as well as “traditional” compilers. To assess optimality, we compare against the optimal depth topology aware QSearch synthesis tool. To assess the quality of solution and scalability for larger circuits we compare directly against the IBM Qiskit [1] synthesis passes. Note that these are based on the UniversalQ [27] top-down synthesis algorithms. Finally, we compare the quality of the circuit generated by QFAST against the output of traditional compilation and mapping with IBM Qiskit.

Evaluation Metrics: We assess the quality of the generated circuits along several metrics: 1) total CNOT gate count; 2) total count of single qubit gates (including R_Z software gates); 3) critical path length, the longest path of gates

in the circuit; and 4) average gate parallelism. The first three metrics have been previously used by synthesis and circuit mapping studies. Average gate parallelism has been previously ignored as a circuit quality metric due to severe scheduling restrictions caused by QPU crosstalk. As our understanding of crosstalk increases, we believe the presence of gate parallelism in circuits will become important. For the purpose of this study, we use a simple measure defined as $\frac{\text{Total Gate Count}}{\text{Critical Path Length}}$.

Besides circuit structure related metrics, we discuss the Hilbert-Schmidt distance of the solution and total compilation time.

Experimental Results: We compare QFAST against state-of-the-art tools for synthesis and circuit compilation. To assess algorithm optimality, we compare against the QSearch optimal depth topology aware synthesis algorithm, for circuits up to four qubits. We also compare against the IBM Qiskit synthesis algorithm for all benchmarks. Another point of comparison is against traditional compilation: in this case we compile and map any available input reference circuits directly with IBM Qiskit.

We evaluated efficacy on two physical chip topologies: fully-connected and linear (nearest-neighbor). Tables 1 and 2 show metrics for all evaluated circuits, ranging from three to seven qubits. These demonstrate the scalability of QFAST. For each benchmark we have access to a reference circuit implementation obtained from third parties, either domain generators or workloads considered by other studies. The columns marked “Mapped” describe the metrics for the reference inputs, when mapped by IBM Qiskit to a particular topology.

For circuits up to four qubits, we can compare directly against QSearch, as shown in Table 1. This allows us to evaluate the optimality of QFAST.

5.1. Circuit Depth

QFAST produces good quality circuits. When compared against traditional compilation and mapping with IBM Qiskit, QFAST produces circuits with an average of $10\times$ fewer CNOT gates and $5.2\times$ fewer $U3$ gates. These are reflected into an average $5.7\times$ decrease of the circuit critical path and an $1.03\times$ better parallelism. When compared against IBM Qiskit synthesis, the resulting circuit critical path is $156\times$ shorter and parallelism is $2\times$ higher.

When compared against QSearch for circuits up to four qubits, although not optimal, QFAST produces good quality circuits: the critical path is $1.19\times$ longer, while the parallelism is $1.09\times$ higher. Note that QFAST is on average $3.55\times$ faster than QSearch.

QFAST handles topology very well. The ratio between the average critical path length when synthesizing to a linear topology and to a fully connected topology is $1.07\times$. The QSearch ratio is $1.06\times$.

Note that QFAST and QSearch are particularly useful in optimizing circuits such as TFIM, where no optimal implementation is apriori known and the circuit grows linearly with each time step simulation of the target sys-

			3 Qubits							4 Qubits							
			fredkin	toffoli	grover	hhl	or	peres	qft3	adder	vqe	tfim-4-1	tfim-4-10	tfim-4-22	tfim-4-60	tfim-4-80	tfim-4-95
CNOTs	All-to-All	Qiskit Mapped	8	6	7	5	6	5	6	10	76	6	60	132	360	480	570
		QFAST	8	8	7	3	8	7	7	15	43	8	14	16	18	14	21
		QSearch	8	6	7	5	7	6	7	12	22	6	12	13	12	15	12
		Qiskit Synthesized	15	9	29	13	11	11	27	66	566	124	218	218	218	218	218
	Linear	Qiskit Mapped	12	13	14	11	11	9	8	20	85	6	60	132	360	480	570
		QFAST	8	8	7	4	8	7	8	36	40	6	10	10	12	12	23
		QSearch	8	8	7	3	8	7	7	14	24	7	12	13	12	13	12
		Qiskit Synthesized	30	17	74	30	19	28	70	247	2630	477	523	523	523	523	523
U3s	All-to-All	Qiskit Mapped	10	8	17	10	9	9	11	11	86	7	70	154	420	560	665
		QFAST	19	19	17	9	19	17	17	34	91	20	32	36	40	32	46
		QSearch	19	15	16	13	17	15	17	26	49	16	28	28	28	31	28
		Qiskit Synthesized	19	11	42	17	17	12	39	88	671	160	261	261	261	261	261
	Linear	Qiskit Mapped	23	22	30	22	22	20	18	37	106	7	70	154	420	560	665
		QFAST	19	19	17	11	19	17	19	76	84	16	24	24	28	28	50
		QSearch	19	19	17	9	19	17	17	32	53	18	28	30	28	30	28
		Qiskit Synthesized	50	32	126	49	37	45	120	410	4169	785	851	851	851	850	851
Depth	All-to-All	Qiskit Mapped	11	11	16	11	8	8	12	11	116	10	73	157	423	563	668
		QFAST	17	17	15	7	17	15	15	21	61	9	21	29	29	29	35
		QSearch	17	13	15	11	15	13	15	19	39	13	21	24	19	27	21
		Qiskit Synthesized	29	17	56	26	21	19	51	121	1062	227	421	421	421	421	421
	Linear	Qiskit Mapped	23	24	29	23	21	18	17	32	136	10	73	157	423	563	668
		QFAST	17	17	15	9	17	15	17	63	63	9	13	21	25	21	31
		QSearch	17	17	15	7	17	15	15	27	41	15	23	23	25	23	21
		Qiskit Synthesized	56	34	139	55	38	51	132	390	3949	770	852	852	852	852	852
Parallelism	All-to-All	Qiskit Mapped	1.64	1.27	1.50	1.36	1.88	1.75	1.42	1.91	1.40	1.30	1.78	1.82	1.84	1.85	1.85
		QFAST	1.59	1.59	1.60	1.71	1.59	1.60	1.60	2.33	2.20	3.11	2.19	1.79	2.00	1.59	1.91
		QSearch	1.59	1.62	1.53	1.64	1.60	1.62	1.60	2.00	1.82	1.69	1.90	1.71	2.11	1.70	1.90
		Qiskit Synthesized	1.17	1.18	1.27	1.15	1.33	1.21	1.29	1.27	1.16	1.25	1.14	1.14	1.14	1.14	1.14
	Linear	Qiskit Mapped	1.52	1.46	1.52	1.43	1.57	1.61	1.53	1.78	1.40	1.30	1.78	1.82	1.84	1.85	1.85
		QFAST	1.59	1.59	1.60	1.67	1.59	1.60	1.59	1.78	1.97	2.44	2.62	1.62	1.60	1.90	2.35
		QSearch	1.59	1.59	1.60	1.71	1.59	1.60	1.60	1.70	1.88	1.67	1.74	1.87	1.60	1.87	1.90
		Qiskit Synthesized	1.43	1.44	1.44	1.44	1.47	1.43	1.44	1.68	1.72	1.64	1.61	1.61	1.61	1.61	1.61
Time (s)	All-to-All	Qiskit Mapped	0.04	0.04	0.05	0.05	0.04	0.08	0.04	0.05	0.36	0.03	0.20	0.40	1.00	1.33	1.67
		QFAST	1.82	1.77	1.82	0.23	4.57	0.54	0.70	7.71	553.79	1.29	13.19	12.26	10.87	6.12	11.29
		QSearch	2.99	1.89	1.84	0.47	1.01	0.60	0.98	34.57	2006.31	10.56	42.59	16.41	31.73	30.71	51.12
		Qiskit Synthesized	0.26	0.14	0.86	0.24	0.22	0.19	0.60	1.58	12.10	2.85	3.36	3.50	3.37	3.52	3.32
	Linear	Qiskit Mapped	0.17	0.15	0.17	0.15	0.16	0.18	0.13	0.20	1.04	0.06	0.32	0.66	1.82	2.54	2.93
		QFAST	1.66	1.64	1.78	0.41	1.60	1.25	1.89	16.25	201.63	0.64	1.77	1.85	3.00	2.81	6.08
		QSearch	2.42	1.62	1.42	0.21	1.52	1.13	0.72	32.61	765.19	1.93	57.15	18.82	9.54	12.80	11.24
		Qiskit Synthesized	0.45	0.28	1.96	0.46	0.37	0.39	1.13	4.07	41.59	7.55	7.02	8.25	6.44	8.47	7.00

TABLE 1: Results for 3-4 qubit synthesis benchmarks.

tem/Hamiltonian. In the result tables, we indicate the number of qubits and the associated time step, e.g. `tfim-6-10`.

5.2. Scalability and Execution Time

For brevity, we only summarize the execution time trends, and note that QFAST scales up to seven qubits. QFAST is roughly $15\times$ slower than IBM Qiskit and $3.55\times$ faster than QSearch. The maximum compilation time observed was 220 minutes for a seven qubit circuit.

An analysis indicates that $> 90\%$ of the execution time is spent in the *decomposition* stage, with rest spent in the *instantiation stage* for synthesizing small blocks. Overall $> 99\%$ of the total execution time is spent in numerical optimization.

The decision to conflate search and numerical optimization pays off in terms of improved scalability, albeit at a small loss in circuit quality. Scalability comes from exploring a reduced number of partial solutions. For example, for

`tfim-4-95`, the partial solution space for QSearch contains 1,594,323 circuits and the algorithm explores 30,460 circuits. In contrast, for the same input problem, QFAST explores 17 partial solutions, respectively.

5.3. Impact of Native Back-end Synthesis

All results in Tables 1 and 2 have been obtained with QFAST decomposing to two-qubit generic gates, each instantiated with KAK as a native synthesis back-end. For brevity, we note that results obtained when replacing KAK with QSearch are identical in terms of circuit quality and execution time.

Composing with QSearch allows us to study the sensitivity to the granularity of decomposition into two- or three-qubit generic blocks. Detailed results are presented in Table 3, and summarized for six and seven-qubit circuits in Table 4. Overall, directly targeting the smallest block possible generates shorter circuits. The reason is best un-

			5 Qubits								6 Qubits						7 Qubits			
			grover5	hlf	mul	qaqa	qft5	tfim-5-10	tfim-5-40	tfim-5-60	tfim-5-80	tfim-5-100	tfim-6-1	tfim-6-10	tfim-6-24	tfim-6-31	tfim-6-51	tfim-7-20	tfim-7-40	tfim-7-100
CNOTs	All-to-All	Qiskit Mapped	48	13	17	20	20	80	320	480	640	800	10	100	240	310	510	240	480	1200
		QFAST	70	13	18	39	46	20	20	24	22	26	12	29	26	24	28	41	*	*
		Qiskit Synthesized	570	870	77	750	580	1025	1025	1025	1025	1025	4006	4474	4474	4474	4474	18653	18653	18653
	Linear	Qiskit Mapped	131	23	22	55	31	80	320	480	640	800	10	100	240	310	510	240	480	1200
		QFAST	60	55	58	69	114	12	18	20	20	21	10	16	20	22	32	24	31	40
		Qiskit Synthesized	2503	2578	760	2692	2622	2791	2791	2791	2791	2791	13155	13365	13365	13365	13365	58316	58316	58316
U3s	All-to-All	Qiskit Mapped	78	8	16	20	29	90	360	540	720	900	11	110	264	341	561	260	520	1300
		QFAST	145	31	41	83	97	45	45	53	49	57	30	64	58	54	62	89	*	*
		Qiskit Synthesized	672	976	87	861	687	1140	1140	1140	1140	1140	4294	4765	4765	4765	4765	19360	19360	19360
	Linear	Qiskit Mapped	235	37	40	93	63	90	360	540	720	900	11	110	264	341	561	260	520	1300
		QFAST	125	115	121	143	233	29	41	45	45	47	26	38	46	50	70	55	69	87
		Qiskit Synthesized	4008	4046	1190	4264	4165	4400	4401	4401	4401	4400	20375	20659	20658	20656	20658	89478	89480	89483
Depth	All-to-All	Qiskit Mapped	85	16	26	32	26	76	286	426	566	706	16	79	177	226	366	152	292	712
		QFAST	123	21	33	65	85	31	33	49	29	39	13	47	29	29	33	47	*	*
		Qiskit Synthesized	1064	1662	138	1451	1089	2008	2008	2008	2008	2008	7872	8841	8841	8841	8841	37048	37048	37048
	Linear	Qiskit Mapped	200	34	40	76	44	76	286	426	566	706	16	79	177	226	366	152	292	712
		QFAST	99	87	77	83	151	17	21	29	21	27	13	17	25	21	45	23	31	49
		Qiskit Synthesized	3799	3933	1115	4061	3924	4236	4236	4236	4236	4236	19074	19495	19495	19494	19494	82915	82915	82915
Parallelism	All-to-All	Qiskit Mapped	1.48	1.31	1.27	1.25	1.88	2.24	2.38	2.39	2.40	2.41	1.31	2.66	2.85	2.88	2.93	3.29	3.42	3.51
		QFAST	1.75	2.10	1.79	1.88	1.68	2.10	1.97	1.57	2.45	2.13	3.23	1.98	2.90	2.69	2.73	2.77	*	*
		Qiskit Synthesized	1.17	1.11	1.19	1.11	1.16	1.08	1.08	1.08	1.08	1.08	1.05	1.05	1.05	1.05	1.05	1.03	1.03	1.03
	Linear	Qiskit Mapped	1.83	1.76	1.55	1.95	2.14	2.24	2.38	2.39	2.40	2.41	1.31	2.66	2.85	2.88	2.93	3.29	3.42	3.51
		QFAST	1.87	1.95	2.32	2.55	2.30	2.41	2.81	2.24	3.10	2.52	2.77	3.18	2.64	3.43	2.27	3.43	3.23	2.59
		Qiskit Synthesized	1.71	1.68	1.75	1.71	1.73	1.70	1.70	1.70	1.70	1.70	1.76	1.75	1.75	1.75	1.75	1.78	1.78	1.78
Time (s)	All-to-All	Qiskit Mapped	0.16	0.05	0.07	0.07	0.11	0.22	0.88	1.19	1.68	2.03	0.04	0.28	0.62	0.80	1.41	0.61	1.28	3.16
		QFAST	3187.40	27.70	86.79	249.15	499.49	79.86	69.38	71.98	77.42	215.13	23.14	618.43	191.99	270.70	684.63	13222.11	*	*
		Qiskit Synthesized	11.61	14.50	2.65	14.61	14.43	14.35	15.04	14.59	14.27	16.52	82.16	62.93	64.10	63.34	64.62	307.57	290.26	286.75
	Linear	Qiskit Mapped	1.12	0.24	0.38	0.46	0.34	0.43	1.75	2.57	3.39	4.31	0.09	0.51	1.30	1.61	2.60	1.17	2.41	6.09
		QFAST	992.38	228.55	213.94	365.15	1901.26	7.67	22.78	26.63	30.28	21.01	5.25	61.68	82.52	408.35	772.39	2524.35	2659.28	8208.44
		Qiskit Synthesized	33.20	34.42	12.38	36.25	38.37	35.93	35.53	32.27	34.11	32.41	170.08	161.25	156.66	161.30	159.81	676.79	676.95	705.01

TABLE 2: Results for 5-7 qubit synthesis benchmarks. (* implies the program timed-out after 12 hours.)

			6 Qubits					7 Qubits		
			tfim-6-1	tfim-6-10	tfim-6-24	tfim-6-31	tfim-6-51	tfim-7-20	tfim-7-40	tfim-7-100
CNOTs	All-to-All	2-Qubit Gates 3-Qubit Gates	12 38	29 47	26 82	24 68	28 84	41 94	* 127	* 169
	Linear	2-Qubit Gates 3-Qubit Gates	10 16	16 28	20 30	22 38	32 62	24 46	31 51	40 64
U3s	All-to-All	2-Qubit Gates 3-Qubit Gates	30 82	64 100	58 170	54 142	62 174	89 195	* 261	* 345
	Linear	2-Qubit Gates 3-Qubit Gates	26 38	38 62	46 66	50 82	70 130	55 99	69 109	87 135
Depth	All-to-All	2-Qubit Gates 3-Qubit Gates	13 57	47 93	29 161	29 119	33 137	47 159	* 223	* 273
	Linear	2-Qubit Gates 3-Qubit Gates	13 25	17 57	25 43	21 59	45 97	23 75	31 75	49 93
Parallelism	All-to-All	2-Qubit Gates 3-Qubit Gates	3.23 2.11	1.98 1.58	2.90 1.57	2.69 1.76	2.73 1.88	2.77 1.82	* 1.74	* 1.88
	Linear	2-Qubit Gates 3-Qubit Gates	2.77 2.16	3.18 1.58	2.64 2.23	3.43 2.03	2.27 1.98	3.43 1.93	3.23 2.13	2.59 2.14
Time (s)	All-to-All	2-Qubit Gates 3-Qubit Gates	23.14 90.41	618.43 1250.79	191.99 2874.59	270.70 1097.66	684.63 529.49	13222.11 26667.53	* 39124.92	* 31699.46
	Linear	2-Qubit Gates 3-Qubit Gates	5.25 13.30	61.68 293.28	82.52 103.57	408.35 722.94	772.39 1153.03	2524.35 4056.87	2659.28 911.26	8208.44 2431.82

TABLE 3: A comparison between QFAST configured with 2-qubit blocks and 3-qubit blocks. (* implies the program timed-out after 12 hours.)

derstood when examining the results for Linear mapping. In this case, we observe a reduction from 94 two-qubit generic blocks to 45 three-qubit blocks required to represent all circuits. This is expected, as three-qubit blocks have higher “computational” power than two-qubit blocks. On the other hand, the three-qubit blocks seem to have too much computational power in this case, as they expand into long subcircuits. Their depth expansion factor (seven CNOT on average) when instantiated into native gates, is not offset by the reduction in the total number of blocks.

	All-to-All		Linear	
	B=2	B=3	B=2	B=3
CNOT	160	709	195	335
Total Blocks	76	81	94	45
Avg. Bl. Len	2.1	8.7	2.07	7.4

TABLE 4: Summary of QFAST configured with 2-qubit blocks and 3-qubit blocks, when compiling six- and seven-qubit benchmarks.

5.4. Validation of Generated Circuits

At synthesis time, the solution quality is assessed using modifications on the Hilbert-Schmidt distance. All solutions evaluated produce circuits that are some small distance away from the input unitary. Qiskit’s synthesis is closest to target with an average distance of 10^{-14} , followed by QSearch with an average of 10^{-12} and by QFAST with 10^{-6} .

To test the quality of the circuits we have run simulations with inputs set to all the standard basis state vectors and 1000 random state vectors. For all circuits with a distance less than 10^{-3} , the average output state fidelity is greater than 0.9999 with ULP difference of 10^{-5} . The average error of two-qubit gates is on the order of 10^{-2} [14], which leads us to believe the threshold chosen for QFAST is fine for the NISQ era.

In the case of QFAST and QSearch, the precision threshold is configurable. For the QSearch results we asked for 10^{-6} and obtained 10^{-12} . The QFAST results have been obtained with 10^{-3} threshold for the decomposition stage, while the back-end synthesis with KAK is precise. If desired, by increasing the threshold during decomposition, users can obtain even better solutions at the expense of running time.

6. Discussion

QFAST improves upon previous synthesis techniques in either quality of solution or scalability: 1) it is much faster than optimal techniques with little loss in circuit quality; and 2) generates much better circuits than fast techniques, with low enough time penalty. Overall, we find the QFAST results encouraging for the future practical use of synthesis in quantum algorithm exploration and optimization in the NISQ era and beyond.

Scalability is always a concern for synthesis algorithms. The current implementation is not parallelized, besides any internal multi-threading parallelism that may be present in

numerical optimizers. Most of the time is currently spent in the *decomposition* stage, which has no intrinsic parallelism. The little time spent in *instantiation* and *recombination* can be reduced, as these are embarrassingly parallel steps on generic gates. For QFAST to improve, advances in the speed of numerical optimization are required, and we are already contemplating GPU based implementations.

A more subtle problem is trying to determine the useful upper bound on circuit size in qubits which synthesis algorithms should handle. *Is seven qubits good enough to use beyond the NISQ era?* Our recent work and QGo algorithm [53], which combines circuit partitioning techniques with synthesis indicates that a practical upper bound may be lower than expected, as we show great depth reduction for circuits up to 100 qubits when using QSearch optimal synthesis on four-qubit blocks. In this context, the expectation is that deploying QFAST will reduce time to solution while improving final solution quality. Furthermore, we expect gradually lower return-on-investments when scaling the bottom algorithms up to more qubits. An indication of the dynamics at work can be seen in the analysis of QFAST behavior with block size.

Examining the behavior of these synthesis algorithms with respect to topology raises some interesting conjectures to help guide users in their choice of the appropriate tool for a given problem. The determining factor seems to be the relationship between the topology and qubit interactions required on the original quantum algorithm side (e.g. QFT, adder), and the topology on the physical QPU side. For bottom-up search based techniques (QSearch), the quality of the solution is not affected by any mismatch, just the time to solution. In this case mapping a low logical connectivity algorithm, such as TFIM, on a rich all-to-all physical connectivity QPU will increase the total time to solution by a large margin. For QFAST, both the quality of the solution and the time to solution are affected. For example, we see a non-intuitive depth inversion when mapping TFIM to an all-to-all physical topology: the solution circuits are longer than when mapping directly to a linear topology. Overall, the results indicate that in practice, when using bottom-up approaches it is probably a good heuristic to map to the most restricted linear topology, irrespective of the physical chip topology. The conjecture is reversed for top-down approaches which seem really challenged by anything other than all-to-all connectivity.

7. Related Work

A foundational result is provided by the Solovay Kitaev (SK) theorem which relates circuit depth to the quality of the approximation [4], [19], [39]. Different approaches [5], [6], [10], [12], [19], [20], [22], [34], [36], [44], [50] have been introduced since, with the goal of generating shorter depth circuits. These can be coarsely classified based on several criteria: 1) target gate set; 2) algorithmic approach; and 3) solution distinguishability.

Target Gate Set: Some algorithms target gates likely to be used only when fault tolerant quantum computing material-

izes. Examples include synthesis of z-rotation unitaries with Clifford+V approximation [42] or Clifford+T gates [3], [32], [41]. While these efforts propelled the field of synthesis, they are not used on NISQ devices, which offer a different gate set (e.g. U_3 , R_x , R_z , $CNOT$ and Mølmer-Sørensen all-to-all). Several [17], [26], [33], [46] algorithms, discussed below target these gates directly. From our perspective, since QFAST is composable and can invoke any synthesizer for instantiation, the existence of these algorithms indicates that QFAST is portable across gate sets.

Algorithmic Approaches: Most earlier attempts inspired by Solovay Kitaev use a recursive (or divide-and-conquer) formulation. More recent search based approaches are illustrated by the Meet-in-the-Middle [5] algorithm. Several approaches [12], [50] use techniques from linear algebra for unitary/tensor decomposition, but there are open questions as to the suitability for hardware implementation because algorithms are expressed in terms of row and column updates of a matrix rather than in terms of qubits.

The state-of-the-art upper bounds on circuit depth are provided by techniques [26], [46] that use Cosine-Sine decomposition. The Cosine-Sine decomposition was first used by [48] for compilation purposes. In practice, commercial compilers ubiquitously deploy only KAK decompositions for two qubit unitaries. Khaneja and Glaser have applied the KAK Decomposition to more than just 2-qubit systems [28]. For a 3-qubit system, it originally required 64 CNOTs [51], which was later reduced to 40 CNOTs [52]. We have shown above that this can be beaten by any of the three synthesis tools tested in this work. IBM Qiskit (based in UniversalQ [26]) is an exponent evaluated in this paper. The basic formulation of these techniques is topology independent. The published approaches are hard to extend to different qubit gate sets.

Several techniques [17], [29], [33] use numerical optimization and report results for systems with at most four qubits. They describe the single qubit gates in their variational/continuous representation and use optimizers and search to find a gate decomposition and instantiation. From these, we compare directly against QSearch [17] which is the only published optimal and topology-aware technique. For our purposes, all these techniques seem to solve a combinatorial number of hard (low distance) optimization problems. We expect QFAST to scale better while providing comparable results. Furthermore, due to its composability, we can directly leverage any of these implementations.

Topology awareness is important for synthesis algorithms, with opposing trends. Most formulations assume all-to-all connectivity. Specializing for topology in linear algebra decomposition techniques seems to increase circuit depth by rather large constants, [46] mention a factor of nine, improved by [26] to $4\times$. Specializing for topology in search and numerical optimization techniques seems to reduce circuit depth and Davis et al [17] report up to $4\times$ reductions. QFAST behaves like the latter.

Solution Distinguishability: Synthesis algorithms are classified as exact or approximate based on distinguishability. This is a subtle classification criteria, as most algorithms can

be viewed as either. For example, [5] proposed a divide-and-conquer algorithm called Meet-in-the-Middle (MIM). Designed for exact circuit synthesis, the algorithm may also be used to construct an ϵ -approximate circuit. The results seem to indicate that the algorithm failed to synthesize a three qubit QFT circuit.

Furthermore, on NISQ devices, the target gate set of the algorithm (e.g. T gate) may be itself implemented as an approximation when using native gates.

We classify our approach as approximate since we accept solutions at a small distance from the original unitary. In a sense, when algorithms move from design to implementation, all become approximate due to numerical floating point errors.

8. Conclusion

We have presented a quantum synthesis algorithm designed to produce short circuits and scale well in practice. QFAST belongs in the class of bottom-up synthesis tools that use numerical optimization. The main contribution is a circuit encoding that allows replacing expansive search over large circuit spaces with a single step of numerical optimization in a topology aware manner. The evaluation on depth optimal circuits, as well as circuits generated by domain generators (VQE, TFIM) indicates that while not optimal, QFAST can significantly reduce the depth of circuits used in practice by domain scientists. This reduction is beyond the capabilities of other existing synthesis tools or optimizing compilers. This bodes well for the future adoption of synthesis for algorithm discovery or circuit optimization during the NISQ era and beyond.

Acknowledgments

This work was supported by the DOE under contract DE-5AC02-05CH11231, through the Office of Advanced Scientific Computing Research (ASCR) Quantum Algorithms Team and Accelerated Research in Quantum Computing programs.

References

- [1] Ibm qiskit. Available at <https://qiskit.org/>.
- [2] Python package index. <https://pypi.org>.
- [3] *Classical and Quantum Computation*. American Mathematical Society, Boston, MA, 2012.
- [4] O. Al-Ta'ani. *Quantum Circuit Synthesis using Solovay-Kitaev Algorithm and Optimization Techniques*. PhD thesis, 2015.
- [5] M. Amy, D. Maslov, M. Mosca, and M. Roetteler. A meet-in-the-middle algorithm for fast synthesis of depth-optimal quantum circuits. *Trans. Comp.-Aided Des. Integ. Cir. Sys.*, 32(6):818–830, June 2013.
- [6] M. Amy and M. Mosca. T-count optimization and Reed-Muller codes. *arXiv:1601.07363v1*, 2016.
- [7] L. Bassman, K. Liu, Y. Geng, D. Shebib, A. Krishnamoorthy, and P. Vashishta. Simulating dynamic material properties on near-term quantum computers. *ulletin of the American Physical Society*, 2020.

- [8] L. Bassman, K. Liu, A. Krishnamoorthy, T. Linker, Y. Geng, D. Shebib, S. Fukushima, F. Shimojo, R. K. Kalia, A. Nakano, et al. Towards simulation of the dynamics of materials on quantum computers. *Physical Review B*, 101(18):184305, 2020.
- [9] C. M. Bishop. *Pattern recognition and machine learning*. springer, 2006.
- [10] A. Bocharov and K. M. Svore. Resource-optimal single-qubit quantum circuits. *Phys. Rev. Lett.*, 109:190501, Nov 2012.
- [11] L. Brančik. Matlab programs for matrix exponential function derivative evaluation. *Proc. of Technical Computing Prague 2008*, pages 17–24, 2008.
- [12] S. S. Bullock and I. L. Markov. An arbitrary two-qubit computation in 23 elementary gates or less. In *Proceedings 2003. Design Automation Conference (IEEE Cat. No.03CH37451)*, pages 324–329, June 2003.
- [13] R. H. Byrd, P. Lu, J. Nocedal, and C. Zhu. A limited memory algorithm for bound constrained optimization. *SIAM Journal on scientific computing*, 16(5):1190–1208, 1995.
- [14] A. D. Córcoles, J. M. Gambetta, J. M. Chow, J. A. Smolin, M. Ware, J. Strand, B. L. T. Plourde, and M. Steffen. Process verification of two-qubit quantum gates by randomized benchmarking. *Phys. Rev. A*, 87:030301, Mar 2013.
- [15] A. Cowtan, S. Dilkes, R. Duncan, W. Simmons, and S. Sivaram. Phase gadget synthesis for shallow circuits. *arXiv preprint arXiv:1906.01734*, 2019.
- [16] A. W. Cross, L. S. Bishop, J. A. Smolin, and J. M. Gambetta. Open quantum assembly language, 2017.
- [17] M. G. Davis, E. Smith, A. Tudor, K. Sen, I. Siddiqi, and C. Iancu. Heuristics for quantum compiling with a continuous gate set. *arXiv preprint arXiv:1912.02727*, 2019.
- [18] M. G. Davis, E. Smith, A. Tudor, K. Sen, I. Siddiqi, and C. Iancu. Towards optimal topology aware quantum circuit synthesis. In *2020 IEEE International Conference on Quantum Computing and Engineering (QCE)*, pages 223–234, 2020.
- [19] C. M. Dawson and M. A. Nielson. The Solovay-Kitaev Algorithm. *Quant. Info. Comput.*, 6(1):81–95, 2005.
- [20] A. De Vos and S. De Baerdemacker. Block-*zzz* synthesis of an arbitrary quantum circuit. *Phys. Rev. A*, 94:052317, Nov 2016.
- [21] D. Deutsch. Quantum computational networks. 425:73–90, 09 1989.
- [22] B. Giles and P. Selinger. Exact synthesis of multiqubit Clifford+T circuits. *Physical Review Letters.*, 87(3):032332, Mar. 2013.
- [23] A. W. Harrow, A. Hassidim, and S. Lloyd. Quantum Algorithm for Linear Systems of Equations. *Physical Review Letters*, 103(15):150502, Oct. 2009.
- [24] P. E. Hart, N. J. Nilsson, and B. Raphael. A formal basis for the heuristic determination of minimum cost paths. *IEEE Transactions on Systems Science and Cybernetics*, 4(2):100–107, July 1968.
- [25] R. Iten, R. Colbeck, I. Kukuljan, J. Home, and M. Christandl. Quantum circuits for isometries. *Phys. Rev. A*, 93:032318, Mar 2016.
- [26] R. Iten, R. Colbeck, I. Kukuljan, J. Home, and M. Christandl. Quantum circuits for isometries. *Physical Review A*, 93:032318, Mar 2016.
- [27] R. Iten, O. Reardon-Smith, L. Mondada, E. Redmond, R. Singh Kohli, and R. Colbeck. Introduction to UniversalQCompiler. *arXiv e-prints*, page arXiv:1904.01072, Apr 2019.
- [28] N. Khaneja and S. Glaser. Cartan decomposition of $su(2^n)$, constructive controllability of spin systems and universal quantum computing. *arXiv preprint quant-ph/0010100*, 2000.
- [29] S. Khatri, R. LaRose, A. Poremba, L. Cincio, A. T. Sornborger, and P. J. Coles. Quantum-assisted quantum compiling. *arXiv e-prints*, page arXiv:1807.00800, Jul 2018.
- [30] V. Kliuchnikov, A. Bocharov, and K. M. Svore. Asymptotically Optimal Topological Quantum Compiling. *Physical Review Letters*, 112:140504, Apr 2014.
- [31] V. Kliuchnikov, D. Maslov, and M. Mosca. Fast and efficient exact synthesis of single-qubit unitaries generated by clifford and t gates. *Quantum Info. Comput.*, 13(7-8):607–630, July 2013.
- [32] V. Kliuchnikov, D. Maslov, and M. Mosca. Practical approximation of single-qubit unitaries by single-qubit quantum clifford and t circuits. *IEEE Transactions on Computers*, 65(1):161–172, Jan 2016.
- [33] E. Martinez, T. Monz, D. Nigg, P. Schindler, and R. Blatt. Compiling quantum algorithms for architectures with multi-qubit gates. *ArXiv e-prints*, July 2016.
- [34] E. A. Martinez, T. Monz, D. Nigg, P. Schindler, and R. Blatt. Compiling quantum algorithms for architectures with multi-qubit gates. *New Journal of Physics*, 18(6):063029, 2016.
- [35] J. R. McClean, J. Romero, R. Babbush, and A. Aspuru-Guzik. The theory of variational hybrid quantum-classical algorithms. *New Journal of Physics*, 18(2):23023, 2016.
- [36] M. Möttönen, J. J. Vartiainen, V. Bergholm, and M. M. Salomaa. Quantum circuits for general multiqubit gates. *Phys. Rev. Lett.*, 93:130502, Sep 2004.
- [37] P. Murali, J. M. Baker, A. Javadi Abhari, F. T. Chong, and M. Martonosi. Noise-Adaptive Compiler Mappings for Noisy Intermediate-Scale Quantum Computers. *arXiv e-prints*, page arXiv:1901.11054, Jan 2019.
- [38] P. Murali, J. M. Baker, A. Javadi-Abhari, F. T. Chong, and M. Martonosi. Noise-adaptive compiler mappings for noisy intermediate-scale quantum computers. In *Proceedings of the Twenty-Fourth International Conference on Architectural Support for Programming Languages and Operating Systems*, pages 1015–1029. ACM, 2019.
- [39] A. B. Nagy. On an implementation of the Solovay-Kitaev algorithm. *arXiv:quant-ph/0606077*, 2016.
- [40] V. NAMIAS. The Fractional Order Fourier Transform and its Application to Quantum Mechanics. *IMA Journal of Applied Mathematics*, 25(3):241–265, 03 1980.
- [41] A. Paetznick and K. M. Svore. Repeat-until-success: Non-deterministic decomposition of single-qubit unitaries. *Quantum Info. Comput.*, 14(15-16):1277–1301, Nov. 2014.
- [42] N. J. Ross. Optimal ancilla-free clifford+v approximation of z-rotations. *Quantum Info. Comput.*, 15(11-12):932–950, Sept. 2015.
- [43] W. Rossmann. *Lie groups: an introduction through linear groups*, volume 5. Oxford University Press on Demand, 2006.
- [44] G. Seroussi and A. Lempel. Factorization of symmetric matrices and trace-orthogonal bases in finite fields. *SIAM Journal on Computing*, 9(4):758–767, 1980.
- [45] V. V. Shende, S. S. Bullock, and I. L. Markov. Synthesis of quantum-logic circuits. *IEEE Transactions on Computer-Aided Design of Integrated Circuits and Systems*, 25(6):1000–1010, 2006.
- [46] V. V. Shende, S. S. Bullock, and I. L. Markov. Synthesis of quantum-logic circuits. *IEEE Transactions on Computer-Aided Design of Integrated Circuits and Systems*, 25(6):1000–1010, June 2006.
- [47] D. Shin, H. Hübener, U. De Giovannini, H. Jin, A. Rubio, and N. Park. Phonon-driven spin-floquet magneto-valleytronics in mos2. *Nature Communications*, 9(1):638, 2018.
- [48] R. R. Tucci. A Rudimentary Quantum Compiler(2nd Ed.). *arXiv e-prints*, pages quant-ph/9902062, Feb 1999.
- [49] R. R. Tucci. An Introduction to Cartan’s KAK Decomposition for QC Programmers. *arXiv e-prints*, pages quant-ph/0507171, Jul 2005.
- [50] J. Urias. Householder factorization of unitary matrices. *J. Mathematical Physics*, 51:072204, 2010.

- [51] J. J. Vartiainen, M. Möttönen, and M. M. Salomaa. Efficient decomposition of quantum gates. *Physical review letters*, 92(17):177902, 2004.
- [52] F. Vatan and C. P. Williams. Realization of a general three-qubit quantum gate. *arXiv preprint quant-ph/0401178*, 2004.
- [53] X.-C. Wu, M. G. Davis, F. T. Chong, and C. Iancu. Optimizing noisy-intermediate scale quantum circuits: A block-based synthesis, 2020.
- [54] A. Younis. Qfast: Quantum synthesis using a hierarchical continuous circuit space. Master's thesis, EECS Department, University of California, Berkeley, May 2020.
- [55] E. Younis, K. Sen, K. Yelick, and C. Iancu. Qfast: Quantum synthesis using a hierarchical continuous circuit space, 2020.